Light scattering and infrared-transmission spike in multidomain birefringent solids (KCN and NaCN)

Michael D. Julian* and Fritz Lüty
Physics Department, University of Utah, Salt Lake City, Utah 84112
(Received 3 August 1979)

KCN and NaCN single crystals, in their low-temperature multidomain structure, are used as model cases for the study of light scattering in polycrystalline birefringent solids. The light-scattering properties, measured over a wide ir range can be fitted to Raman's model, based on the phase shifts of the light in birefringent domains of different orientation, yielding an estimate on the domain sizes. A narrow transmission window in the light-scattering spectrum is observed in the near ir, where the otherwise opaque and light-depolarizing crystal is nearly perfectly transparent and nondepolarizing. This effect can be quantitatively understood as a matching between birefringence from electronic and vibrational excitation, producing an effective optically isotropic behavior of the molecular system at a particular wavelength. Consequences of this birefringence-matching effect for other molecular systems and experimental techniques are discussed.

Polycrystalline solids, formed from transparent birefringent single crystals, are known to be opaque and light scattering. This is due to the refractive-index mismatch between domains of different orientations, leading to reflection, refraction, diffraction, and depolarization of the incoming light. Quartz, calcite, and *gypsum*, in their polycrystalline mineral forms as quartzite, marble, and alabaster, are well-known examples. The size of the birefringence Δn determines strength and nature of the light attenuation: For strongly birefringent materials, *light reflection* will be predominant (producing, for instance, in calcite the brillant white appearance of marble), while for weakly birefringent materials *light scattering* (with often strong wavelength dependence) will be predominant.

We have observed—to our knowledge for the first time—that in the smooth spectral attenuation curves of these materials *sharp transmission spikes* can occur, so that the otherwise opaque material becomes optically transparent to light of a particular wavelength λ_s. This is due to a special form of the *Christiansen effect*, involving refractive-index matching in optically inhomogeneous media.[1] In the usual type of Christiansen filter, small transparent particles (like glass) of refractive index $n_1(\lambda)$ are suspended in a suitable transparent liquid of refractive index $n_2(\lambda)$. For all wavelengths λ at which $n_1 \neq n_2$ the mixture is optically inhomogeneous and scatters light. For a wavelength λ_s at which the two dispersion curves intersect, however, the mixture becomes optically homogeneous and thus transmits light [Fig. 1(a)]. Christiansen filter systems with sharp transmission spikes in the visible and infrared range have been produced by numerous liquid-solid mixtures,[2] often tuneably via the strong dependence of the liquid's refractive index on temperature[3] or small chemical additives.

We demonstrate here the existence of Christiansen effects in *pure polycrystalline birefringent solids* using potassium cyanide and sodium cyanide as model systems. These materials stand as representatives for an extended class of ionic crystals, of the type $M^+(XY)^-$, built from a metal point-ion M^+ and a diatomic molecular ion $(XY)^-$—KOH, NaSH, and TlCN are some other examples. Materials of this composition are in most cases pseudocubic at high temperatures due to reorientational averaging out of the molecular anisotropies. By cooling to low temperatures, these orientationally disordered crystals undergo transitions into phases of various molecular order. Our model systems KCN and NaCN transform at 168 and 288 K, respectively, by a first-order transition into an orthorhombic structure, in which the CN^- molecules align parallel (along the six $\langle 110 \rangle$ orientations of the cubic crystal[4]). Due to the strong elastic distortions involved (the cubic angle changes by 11° and 14°), the single crystal breaks up into a *multidomain structure*, as illustrated schematically in Fig. 2.

Due to the anisotropic polarizability of the CN^- molecules, these domains are birefringent with optical axis along the six equivalent $\langle 110 \rangle$ domain axes. The birefringent behavior of the single domain (or, in fact, of a single CN^- molecule) is determined by two fundamental optical excitations, the electronic (or excitonic) excitation ν_0(elect) in the uv, and the optically active stretching ν_0(vibr) in the ir at ~5 μ. Both these excitations are polarized essentially along the CN^- axis, so that the Kramers-Kronig related $\Delta n(\nu) = n_{\parallel} - n_{\perp}$ curve will qualitatively have a form as illustrated in Fig. 1(b). This composite $\Delta n(\nu)$ curve will

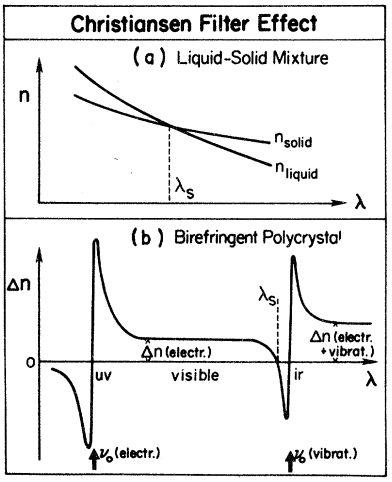

FIG. 1. Dispersion curves for refractive indices (a) and birefringence (b) of light-scattering systems, which exhibit a Christiansen effect at λ_s.

determine spectral light-scattering properties of the multidomain cyanide crystal: Depending of the size of $\Delta n(\nu)$, light will be scattered due to the refractive-index mismatch between the differentially oriented domains $A-F$, as indicated in Fig. 2.

Figure 3 shows ir transmission spectra of a thin

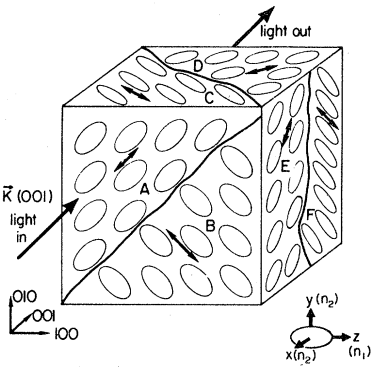

Light Polarization	Domains	Refractive Index	Depolarization Effect
[100]	A, B	$\frac{1}{2}(n_1+n_2)$	# 2
	C, D	$\frac{1}{2}(n_1+n_2)$	3
	E, F	n_2	1
[110]	A	n_1	1
	B	n_2	1
	C, D, E, F	$\frac{1}{4}(n_1+3n_2)$	4

FIG. 2. Schematic illustration of the domain structure of KCN with the CN^- molecules (and their refractive index ellipsoids) parallel ordered along the six ⟨110⟩ directions of the originally cubic crystal. The table indicates the six domain orientations with their different refractive indices and depolarization effects for ⟨100⟩- and ⟨110⟩-polarized light.

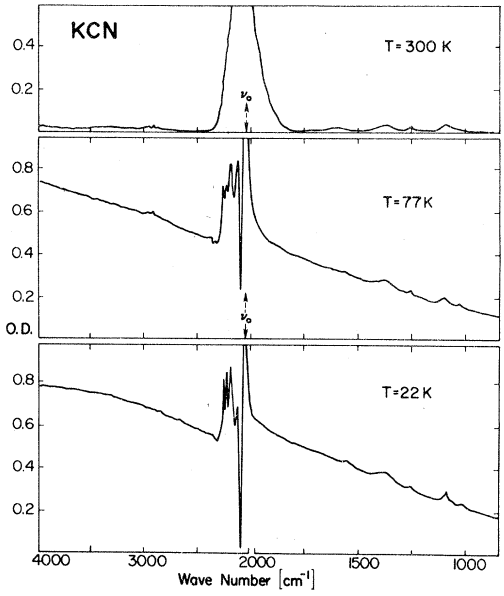

FIG. 3. Infrared transmission spectrum of a thin crystal of KCN, measured at three different temperatures.

KCN crystal at three temperatures. At RT (in the pseudocubic phase) the crystal is completely transparent outside the spectral region of the stretching band at ν_0 (the peak of which is far out of scale). Under cooling through the disorder-order phase transition, the crystal develops strong light attenuation (increasing towards shorter wavelengths) due to light scattering by the multidomain structure. The band due to the CN^- stretching vibration ν_0 narrows under cooling, and a sharp multiline structure at its high-energy side, due to the excitation of (stretching + vibration) combination modes, becomes detectable. The most outstanding and astonishing effect, however, is the appearance of a sharp transmission spike very close to the high-energy side of the CN^- stretch band. It becomes very pronounced under cooling, so that at lowest temperatures the opaque crystal becomes nearly completely transparent around $\nu = 2089\ cm^{-1}$. Figure 4 displays two similar measurements for NaCN, taken at RT in the pseudocubic and at 10 K in the multidomain structure. In the latter case, again a transmission spike in the light-attenuation spectrum appears at 2110 cm^{-1} on the high-energy side of the stretching absorption band. Figure 5 shows a high-resolution spectrum of the transmission spike in KCN, measured with unpolarized light (a) and with polarizer and analyzer parallel and crossed along ⟨100⟩ and ⟨110⟩ direction (b) and (c). The polarized measurements show that in the center of the spike the light (which is other-

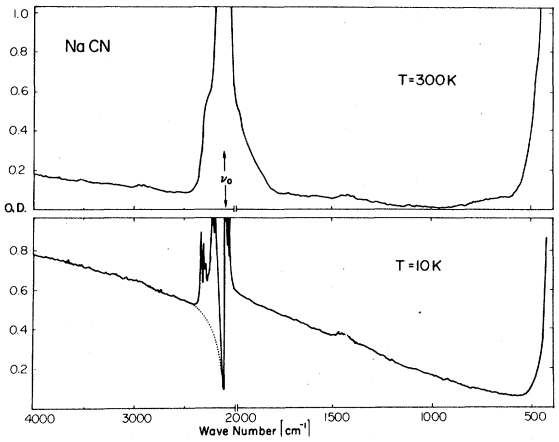

FIG. 4. Infrared transmission spectrum of a NaCN crystal, measured at 300 and 10 K.

wise scattered and depolarized) is traversing the crystal essentially unattenuated and under preservation of its polarization.

This amazing singularity in the light-scattering and depolarization properties of the material at ν_s can only be caused by a *vanishing birefringence* $\Delta n = 0$ for *all* domains so that they are no longer optically distinguished. From the composite electric and vibrational $\Delta n(\nu)$ curve in Fig. 1(b), such a $\Delta n = 0$ point is indeed predicted to lie at ν_s on the high-energy side of ν_0(vibrat). The condition for ν_s is given by

$$\Delta n(\nu_s) = \Delta n(\text{electr}) + \Delta n(\text{vibrat}) = 0 . \tag{1}$$

The electronic part can be estimated from Kerr-effect measurements on *dilute* systems of CN^- molecules substituted into alkali halides, in which the refractive index change under field alignment of the CN^- dipoles was directly measured.[5] Extrapolation of these data on dilute CN^- systems to pure KCN leads to the prediction that a single domain of KCN with parallel ordered CN^- should have in the visible and near ir range a birefringence of $\Delta n(\text{electr}) = n_{\parallel} - n_{\perp} = 0.037$. The refractive-index contribution from the stretching absorption at ν_0(vibrat) is given by the Kramers-Kronig relation to be (outside the band)

$$n(\text{vibrat}) = \frac{A}{2\pi^2(\nu_0^2 - \nu^2)} , \tag{2}$$

where A is the integrated absorption. The birefringence for a fully aligned system of these linearly polarized stretching oscillators would therefore be $\Delta n(\text{vibrat}) = n_{\parallel} - n_{\perp} = 3n(\text{vibrat})$. The condition for the Christiansen effect $\Delta n_{\text{total}}(\nu_s) = 0$ thus yields

$$\nu_s^2 - \nu_0^2 = \frac{3A}{2\pi^2 \Delta n(\text{electr})} , \tag{3}$$

or with $\nu_s^2 - \nu_0^2 \approx (\nu_s - \nu_0)2\nu_0$,

$$\nu_s = \nu_0 + \frac{3A}{2\pi^2 \times 2\nu_0 \times \Delta n(\text{electr})} . \tag{4}$$

Extrapolating—from measurement on dilute KCN KCL:KCN systems—the area A of the vibrational absorption (at $\nu_0 = 2074\ \text{cm}^{-1}$) and the Kerr-effect Δn(electr) results to pure KCN, yield a prediction for the position of the transmission spike at $\nu_s = 2017\ \text{cm}^{-1}$. The agreement to the observed $\nu_s = 2089\ \text{cm}^{-1}$ value is quite good, regarding the inherent uncertainties in the estimated A and Δn(electr) values: Deviations from an exact additive scaling of the A and Δn(electr) values with the CN^- concentration, and uncertainties in electric dipole and local-field-correction values in the Kerr-effect results can easily explain the small deviation.

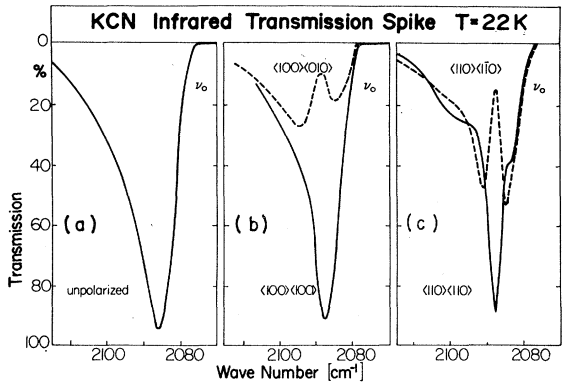

FIG. 5. High-resolution spectrum of the transmission spike at 2088 cm^{-1}, measured unpolarized (a) and with polarizer and analyzer parallel and crossed along ⟨100⟩- and ⟨110⟩-directions (b) and (c).

The occurrence of the transmission spike, by matching of the electronic and vibrational anisotropies at ν_s, does *not* depend on the particular mechanism (reflection, refraction, or diffraction) by which the light is scattered and attentuated in the multidomain structure. In our weakly birefringent material it is very likely that diffraction (phase) effects are predominant in producing the scattering. A simplified model, in which the crystal (of thickness D) is divided into cubic blocks of equal size d with two different refractive indices n_1 and n_2 as developed and discussed by Raman and coworkers,[6] is illustrated in Fig. 6. Neglecting reflection and refraction effects, this "three-dimensional phase grating" will produce—due to the statistically fluctuating distribution of the n_1 and n_2 blocks—phase shifts between the pencils of light, which transmit a row of D/d domains (see Fig. 6.) As a consequence of this, diffracted

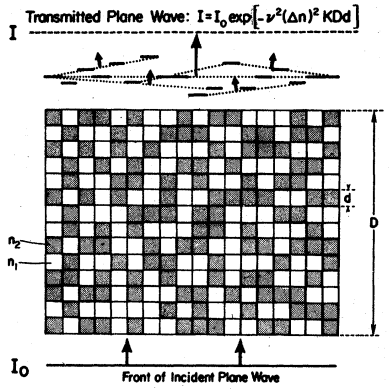

FIG. 6. Schematic illustration of simple model for light scattering in optically inhomogeneous material (see text).

wave fronts emerge behind the crystal in various directions, producing a "scattering halo." The incident plane wave of intensity I_0 emerges in its original direction with an attenuated intensity I, which for small $\Delta n = n_1 - n_2$ is given by

$$I = I_0 \exp(-\nu^2\pi^2\Delta n^2 K \times D \times d)\,, \tag{5}$$

where the "filling factor" K is determined by the relative amount of the n_1 and n_2 blocks ($K_{\max}=1$ for equal amounts). Using this formula and the predicted $\Delta n(\nu)$ from Eq. (4), we obtain a calculated optical-attenuation spectrum as shown by the dotted line in Fig. 7 (fitted to give the observed ν_s - transmission-spike position). Comparison to a measured attenuation spectrum (full line in Fig. 7)

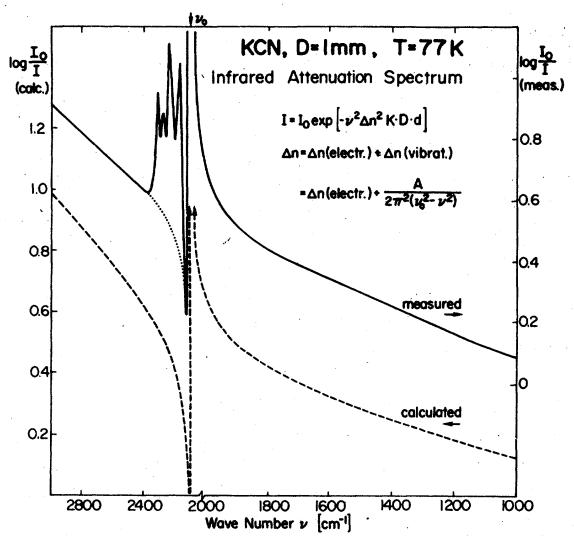

FIG. 7. Measured infrared spectrum of a KCN crystal of 1 mm thickness, in comparison to the calculated behavior obtained from a model, described in the text.

shows that the overall scattering behavior (which increases with ν^2) is rather well represented by this model. The presence of the vibrational sideband structure on the Stokes side of the stretching absorption band interferes with the transmission spike and prevents an exact determination of its spectral structure. The calculated curve shows that the spike should be much more unsymmetric, with a gradual tapering-off towards higher wave numbers.

It should be noted that a normal transmission measurement (as done in our case in a Beckman 4220 infrared spectrophotometer) is not able to separate completely the attenuated original wave from the scattered waves. Due to the finite acceptance angle of the instrument, light which is scattered by a small angle within this "cone of acceptance" will still reach the detector and contribute to the transmitted signal. This will tend to decrease the slope of the spectral-attenuation curves (Figs. 3, 4, and 7) and can, in particular, explain the deviation from the calculated behavior toward high wave numbers (i.e., large attenuation).

In spite of these experimental uncertainties and the oversimplification of the Raman model, a quantitative comparison of measured and calculated behavior is useful in order to obtain an estimate on the (completely unknown) domain size. Using an effective Δn value and filling factor K appropriate for our system, we obtain from the absolute fit between measurement and theory (Fig. 7) a value of $d \approx 80\ \mu$m. This absolute value should be regarded only as a rough estimate on the mean size of the birefringent domains.

The Raman model may be extended to treat the scattering of polarized light. The measurements in Fig. 5 show, that $\langle 110\rangle$ polarized light is attenuated more strongly than $\langle 100\rangle$ polarized light under tuning of ν away from ν_s. The following argument will derive a different filling factor K for each polarization direction, supporting this result.

From Fig. 2 one finds average effective indices of refraction for the various polarizations and domain symmetries. These expressions follow from the fact that $n_1 \approx n_2$ and that $\epsilon = n^2$, where ϵ is the dielectric constant. Once it is realized that the Raman model is a random-walk (in phase) problem, further results can be developed from statistical reasoning.

Let n_i' be the index of refraction from domain i, p_i the probability of encountering such a domain, and m the number of different types of domains (here, $m=6$). (All domains are considered to have the same size.) The average index refraction throughout the crystal is

$$n = \sum_{i=1}^{m} p_i n_i' . \tag{6}$$

Taking this average n as a reference point, one may define the biased index of refraction for each domain as $n_i = n_i' - n$. The random-walk phase step is then given by $\phi_i = 2\pi\nu n_i d$. The variance in phase step for a single domain is given by

$$\sigma_d^2 = \sum_{i=1}^{m} p_i \phi_i^2 = 4\pi^2\nu^2 d^2 \sum_{i=1}^{m} p_i n_i^2 . \tag{7}$$

The variance σ^2 for a light path of length D is just the sum of the variances. Thus,

$$\sigma^2 = N\sigma_d^2; \quad \text{where } N = D/d . \tag{8}$$

By the law of large numbers, the probability distribution of phase is Gaussian. The distribution function is

$$f(\phi) = \frac{1}{\sqrt{2\pi\sigma^2}} \exp(-\phi^2/2\sigma^2) . \tag{9}$$

The effective wave vector of the emergent light is then

$$\psi = \langle e^{i\phi} \rangle = \int_{-\infty}^{\infty} f(\phi) e^{i\phi} d\phi . \tag{10}$$

The emergent light intensity then becomes

$$I = I_0 |\psi|^2 = I_0 e^{-\sigma^2} . \tag{11}$$

In our specific cases

$$I_{\langle 100 \rangle} = I_0 \exp(-\tfrac{2}{9}\pi^2\nu^2 D\Delta n^2 d) \tag{12}$$

and

$$I_{\langle 110 \rangle} = I_0 \exp(-\tfrac{7}{18}\pi^2\nu^2 D\Delta n^2 d) . \tag{13}$$

The predicted ratio of attcnuation constants K is $K_{110}/K_{100} = 1.75$. This agrees with the result from Fig. 5 that $\langle 110 \rangle$ light attenuates faster than $\langle 100 \rangle$ light in the region of the transmission spike.

The treatment of *light depolarization* in our optically inhomogeneous and birefringent material is much more difficult—and no model is available as yet. In Raman's treatment[6] it was argued (without proof) that both the transmitted attenuated plane wave and the scattered waves would keep their original polarization, even if the domains are birefringent and incident light of arbitrary linear polarization is used. This is definitely *not* observed in our system, where light attenuation by scattering is found to be always accompanied by light depolarization.

The complexity of the depolarization problem can be seen if we consider a light wave of polarization vector $\vec{E}$ and propagation vector $\vec{K}$, incident on uniaxial crystal domains, which are characterized by an optical axis $\vec{z}$ and a plane xy perpendicular to $\vec{z}$. Four different effects will occur, depending on the geometry:

(1) *No light depolarization*, if $\vec{E}$ coincides with $\vec{z}$ or lies in the xy plane.

(2) *Splitting into two orthogonally polarized phase-shifted components* (ellipticity), if $\vec{E}$ forms an angle (other than 0° and 90°) with $\vec{z}$, and $\vec{K}$ lies in the xy plane.

(3) *Change of propagation direction* $\vec{K}$ *without light depolarization* (extraordinary beam) if both $\vec{E}$ and $\vec{K}$ form an angle other than 0° and 90° with $\vec{z}$, but lie in a plane containing $\vec{z}$.

(4) *Splitting into two beams of different* $\vec{K}$ *and* $\vec{E}$ (ordinary and extraordinary beam), if both $\vec{E}$ and $\vec{K}$ of the incident light form an angle other than 0° and 90° with $\vec{z}$ and don't lie in a plane containing $\vec{z}$.

In Fig. 2 is indicated how these optical effects (1)–(4) are produced for $\langle 100 \rangle$- and $\langle 110 \rangle$-polarized light by the presence of the six different domains A–E.

Our transmission window around ν_s allows us to observe, at least qualitatively, how the incident-light geometry and domain birefringence Δn affect the light depolarization. It is evident that at the wave number of maximum transmission ν_s (when $\Delta n \approx 0$) both $\langle 100 \rangle$- and $\langle 110 \rangle$-polarized incident light preserve essentially their polarization (Fig. 5). A spectral variation around ν_s (towards increasing $|\Delta n|$) shows the strong light-depolarization effects of the material, which transfer intensity from the polarized into the depolarized component (Fig. 5). This leads in the transmission spectrum to a sharp decrease of the polarized component, and a *complimentary* initial *increase* of the depolarized component.

The disappearance of the molecular polarizability anisotropy at ν_s, as observed here via the disappearance of light scattering and depolarization in multidomain KCN, should not be limited to this material and to this mode of observation. The $\Delta n(\lambda)$ curve in Fig. 1(B) is in fact basically a characteristic of the *individual molecule* (here CN^-). Due to the approximate additivity of the molecular polarizabilities, this $\Delta n(\lambda)$ behavior should hold for any concentration, and any regular or irregular distribution of molecules in solid, liquid, or gaseous form. The position ν_s of the $\Delta n = 0$ point will lie on the *high-energy* (anomalous-dispersion) side of the vibrational absorption, if both electronic and vibrational polarizability anisotropies have the *same* sign (as here for CN^-, which is for both excitations more polarizable along its axis). For OH^- molecules, on the other hand, which are known from Kerr-effect measurements[7] to have a negative electronic polarizability anisotropy $(n_1 - n_2 < 0)$ but keep, of course, a positive Δn ef-

fect for their stretching vibration, the $\Delta n(\nu_s) = 0$ point is expected to lie on the *low-energy* side of their stretching vibration ($\nu_0 \approx 2.7\ \mu$). With the knowledge of sign and size of the electronic polarizability anisotropy, and the position, strength, and polarization of the molecular vibration, the ν_s point is predictable for each molecule. [If electronic and vibrational Δn effects are very different in size, the composite $\Delta n(\nu)$ curve, Fig. 1(b), may not intersect the $\Delta n = 0$ line.]

Observation of the $n(\nu_s) = 0$ effect is not limited to the disappearing of light scattering due to the *static* arrangements in the multidomain structure, as discussed here. Any elastic or inelastic light-scattering or depolarization effect due to the molecular rotation, vibration, or orientational tunneling, should disappear at ν_s. With the availability of tuneable ir lasers it could become very easy and interesting to study these ν_s points in the infrared, at which molecules lose their polarizability anisotropies, and thus behave optically like spherical particles without any orientational properties.

Stimulating discussions with Professor J. Ball and Dr. P. Gash on the theory of light scattering in inhomogeneous media are gratefully acknowledged. This work was supported by NSF Grants Nos. DMR-74-13870-AOZ and DMR-77-12675.

---

*Present address: Hughes Aircraft Co., Bldg. R1/B210, Los Angeles, CA 90009.

[1]C. Christiansen, Ann. Physik. Chem. 23, 298 (1884) and 24, 439 (1885).
[2]L. Auerbach, Am. J. Phys. 25, 440 (1957).
[3]M. Cloupeau and S. Klarsfeld, Appl. Opt. 12, 198 (1973).
[4]H. Suga, T. Matsuo, and S. Seki, Bull. Chem. Soc. Jpn. 38, 1115 (1965).
[5]A. Diaz-Gongora and F. Lüty, Phys. Status Solidi B 86, 127 (1978).
[6]C. V. Raman and K. S. Viswanathan, Proc. Indian Acad. Sci. A41, 37 (1955).
[7]G. Zibold and F. Lüty, J. Nonmetals 1, 1 (1972).